ANALYSIS OF AN AIRCRAFT DEPARTURE AND SPIN CHARACTERISTICS USING NASH EQUILIBRIUM THEORY

Chao Yan, Lianghui Tu, Yang Yang, Yuhao Wang

School of Aircraft Engineering, Nanchang Hangkong University, China

corresponding author Lianghui Tu, e-mail: 71016@nchu.edu.cn

The departure characteristics and steady-spin characteristics of a training aircraft are analyzed. The sideslip departure characteristics of the aircraft under the maximum weight and the minimum weight are obtained, respectively. When predicting the steady-spin, the equilibrium point of the spin is found by an analytic-graphic method based on "Nash equilibrium theory", and the steady-spin parameters of this aircraft are obtained under the conditions of maximum weight and minimum weight, left spin and right spin, neutral controls and pro-spin controls. The simulation results have good theoretical significance for the optimization and improvement of the aircraft in the preliminary design stage.

Keywords: departure characteristics, spin characteristics, spin equilibrium point

Nomenclature

m	–	Aircraft mass
b	–	Wing span
c	–	Mean aerodynamic chord
g	–	Gravitational acceleration
S	–	Wing area
V	–	Free-stream velocity
R	–	Radius of spin
F_c	–	Lateral force
C_D, C_L	–	Coefficient of lift and drag
$C_{n\beta D}$	–	Sideslip departure parameter
C_{ka}, C_{ki}	–	Moment coefficient of aerodynamic and inertia
$C_{l\beta}, C_{n\beta}$	–	Body-axis aerodynamic rolling and yawing moment due to sideslip
Ω	–	Aircraft conical rate
ΔH	–	Altitude lost in turn
Δt	–	Time in turn
ρ	–	Air density
α	–	Angle of attack, AOA
α_{sd}	–	Angle of attack at sideslip departure
β	–	Angle of sideslip
ψ	–	Euler yaw angles
$\delta_a, \delta_e, \delta_r$	–	Aileron, elevator, rudder deflection
τ	–	Non-dimensionalized wind-axis rotation rate, $\tau = \Omega b/2V$
$\omega_x, \omega_y, \omega_z$	–	Body-axis pitching, rolling and yawing rate
$\dot{\omega}_x, \dot{\omega}_y, \dot{\omega}_z$	–	Derivative of pitching, rolling and yawing rate
I_{xx}, I_{yy}, I_{zz}	–	Moment of inertia
I_{xy}, I_{yz}, I_{zx}	–	Products of inertia
M_x^A, M_y^A, M_z^A	–	Aerodynamic moment components about body axes

1. Introduction

The essence of spin is a curved flight state formed by strong interaction of longitudinal and lateral forces and moments. Despite the continuous development of the aviation industry, the complicated and dangerous spin has not disappeared. Frequent flight accidents caused by aircraft entering the spin in recent years have been made pilots, particularly civil pilots, fearful of the spin. Therefore, researchers should constantly dig deep into the spin mechanism, investigate the spin characteristics, and take preventive measures. The research on spin includes spin mechanism analysis (Bennett and Lawson, 2018; Collins and Sable, 2015), unsteady aerodynamic modeling at high angles of attack (Kou and Zhang, 2021; Mokhtari and Sabzehparvar, 2018), departure characteristics and spin sensitivity analysis (Stenfelt and Ringertz, 2013; Farcy *et al.*, 2020), spin characteristics prediction (Malik *et al.*, 2017), design of spinning control laws (Rogalski *et al.*, 2020), spin recovery and spin prevention measures (Figat and Goraj, 2016; Kapuscinski *et al.*, 2020), etc.

Wind tunnel data is the basis for predicting high angles of attack, stall and spin. Using wind tunnel test data, a differential equation model or neural network can be established to simulate the complicated and unsteady aerodynamic effect during spinning (Abramov *et al.*, 2004; Ignatyev and Khrabrov, 2015). From the high angle of attack to the stall and finally to the spin, the aerodynamic characteristics can be simulated based on the data of the high angle of attack static force test, forced oscillation test and rotary balance test in the low-speed wind tunnels. The dynamic motion characteristics of the spin in the unstable stage are analyzed using unsteady aerodynamic wind tunnel testing techniques such as rotary balance oscillatory coning motion tests and large-amplitude forced oscillation dynamic wind tunnel tests (Cummings *et al.*, 2018; Lee *et al.*, 2019).

There will be a divergent and large-scale non-command motion for the aircraft, that is, departure. When the aircraft enters departure, there exist dangerous actions such as wing swaying, nose pitching-down and shaking. If the recovery process takes too long, the aircraft will most likely enter a spin. Mature departure prediction criteria include the lateral control departure parameter $LCDP$, the sideslip departure parameter $C_{n\beta D}$, the "$\beta + \delta$" stability indication, Weissman ($LCDP - C_{n\beta D}$) and Kalviste criteria. The application scenarios of each criterion are different, e.g., when a yaw departure occurs, the sideslip departure parameter $C_{n\beta D}$ can be applied, and when pitching and yawing departures are coupled, the Kalviste criterion, a stability criterion considering longitudinal and lateral motion coupling effect and aerodynamic nonlinear characteristics, is applied.

At present, the commonly used spin prediction methods include the simplified six-degree-of--freedom equation of motion and nonlinear bifurcation analysis (Sibilski and Wróblewski, 2012). For different types of spins, their prediction methods are different. If the lateral angular velocity is constant, the rotation direction of the aircraft is constant, and the pilot does not clearly feel that the aircraft stops rotating, the aircraft is in a steady-spin. For the prediction of steady--spin, the relationship between the triaxial moment coefficient and is needed, and the solutions are mainly numerical analysis and the analytical graphic method (Bihrle and Barnhart, 1983). However, the disadvantages of the two methods are also clear. The numerical method necessitates a large initial value, which can result in an incorrect or missing solution. The graphic method is fast, but the accuracy of the equilibrium point is not high enough.

Based on the wind tunnel test data of a specific aircraft, including static force test data and rotary balance test data, the departure characteristics and steady-spin characteristics of the aircraft in the range of α from 0° to 90° are analyzed. Using the sideslip departure parameter $C_{n\beta D}$, the departure characteristics of the aircraft in the range of the positive AOA are obtained; when predicting the steady-spin, the equilibrium point of the spin is found by an analytic graphic

method based on "Nash equilibrium theory", and the steady-spin parameters of this aircraft under several different conditions are obtained.

2. Basic theories

2.1. Departure prediction

$C_{n\beta D}$ is used to predict whether the aircraft will have a high probability of yaw departure at high AOA, and its expression (Chambers, 1969) is

$$C_{n\beta D} = C_{n\beta} \cos \alpha - \frac{I_{zz}}{I_{xx}} C_{l\beta} \sin \alpha \tag{2.1}$$

At different AOAs, $C_{n\beta D}$ combines the static derivative of directional stability, the static derivative of lateral stability, and the moment of inertia, which can more realistically reflect the stability of the aircraft direction. The judgment criteria are:

$C_{n\beta D} > 0$, the directional stability is secured, and placed in steady region;

$C_{n\beta D} = 0$, the aircraft begins to lose directional stability, the sideslip departure will occur, and the corresponding AOA is α_{sd};

$C_{n\beta D} < 0$, there is no directional stability, placed in unsteady region, and yawing divergence occurs.

2.2. Prediction of steady-spin

When steady-spin occurs, the pitching, rolling and yawing moments in aerodynamics must balance their respective inertial moments at the same time. Since most of the mass of a modern aircraft is concentrated in the fuselage, the inertial pitching moment causes the nose to pitch up, which means that $q > 0$. The aircraft in steady-spin is in vertical rotation, and always produces a positive inertial pitching moment, so a negative aerodynamic pitching moment must exist in order to achieve the equilibrium. In order to keep the aircraft spinning, there must be an aerodynamic torque that can provide the drive. In the stalling and post-stalling AOA regions, the rolling moment is the dominant driving force for rotation around the velocity vector, but as the AOA increases to a flatter rotational attitude, the yawing moment becomes the dominant term.

In the steady-spin prediction, first the aerodynamic moment curves and the inertia moment curves are made, then the required equilibrium points are found from the intersections of the curves, and finally the complete steady-spin equilibrium solution is obtained by calculation.

3. Analytical graphic method based on Nash equilibrium theory

Game theory is a mathematical theory and method to describe a mathematical model containing contradictions, conflicts, confrontations and cooperation in the real world. It has penetrated into many aspects of social and scientific research and gradually formed an independent and complete theoretical system (Churkin *et al.*, 2021). It is the mutual game of the aerodynamic moment and the inertia moment in the steady-spin. When the strategies of both sides of the game are consistent, an equilibrium is reached.

Nash equilibrium is a typical form of non-cooperative game solution. Through the competitive selection process among all the players, the corresponding benefits of all the players are actively realized, and finally a systematic equilibrium can be achieved in the overall benefits. Nash's main idea is: in a multi-objective game $G = \{S_1, S_2, \ldots, S_m; F_1, F_2, \ldots, F_m\}$, the set

$(s_1^*, s_2^*, \ldots, s_m^*)$ composed of one strategy of each player, the strategy s_i^* of any player i is the best strategy compared with the other players $(s_1^*, \ldots, s_{i-1}^*, s_{i+1}^*, \ldots, s_m^*)$, then $(s_1^*, s_2^*, \ldots, s_m^*)$ is a Nash equilibrium of G.

Based on Nash equilibrium theory, the aerodynamic moment coefficient C_{ka} and inertia moment coefficient C_{ki} are taken as the game players ($k = l, m, n$, the same below), and the equilibrium solution of the coefficients is taken as the iterative strategy $\Delta S_k^w = (\Delta S_k^1, \ldots, \Delta S_k^w)$, and the variable group $(\alpha, \beta, \Omega, V)$ exists in the iterative strategy as the strategy space. More, define the payoff function as

$$\min f_u = |C_{ka} - C_{ki}| \qquad u = 1, 2, 3 \tag{3.1}$$

The specific steps are as follows:

    a. Construct the initial iteration strategy group $\Delta S_m^w = (\Delta S_m^1, \ldots, \Delta S_m^w)$, the iteration strategy is taking α and β as an parameters, and τ as independent variable.

    b. Execute the payoff function: $\min f_1 = |C_{ma} - C_{mi}|$, according to the strategy group.

    c. Set a new iteration strategy group $\Delta S_l^w = (\Delta S_l^1, \ldots, \Delta S_l^w)$, the new iteration strategy is taking β as an independent variable and α as a parameter variable, and combined with τ, also the strategy space in the new strategy group is the variable group obtained by the previous payoff function

    d. Execute the payoff function: $\min f_2 = |C_{la} - C_{li}|$, according to the strategy group.

    e. Set a new iteration strategy group $\Delta S_n^w = (\Delta S_n^1, \ldots, \Delta S_n^w)$, and there is no new iteration strategy in this iteration group, and the strategy space in the new strategy group is the variable group obtained by the previous payoff function.

    f. Execute the payoff function: $\min f_3 = |C_{na} - C_{ni}|$, according to the variable group.

Based on Nash equilibrium theory, it will be more direct to reflect the balance between the aerodynamic moment coefficient and inertia moment coefficient in the form of a payoff function. What is more, after modeling the state equation by this method, the system state and time-varying parameters are placed separately, which is convenient for subsequent program drawing.

4. Mathematical modelling

4.1. Equilibrium equations for forces and moments

After the aircraft entered a steady-spin, the average value of the rotation direction and the rotation angular rate remained unchanged, the aircraft descended rapidly along a small radius helical trajectory, and the spin axis almost coincided with the plumb line. A steady-spin is a dynamic equilibrium motion process, it can be expressed in Fig. 1. During this process, it can be assumed that (1) lateral force is equal to zero; (2) drag is equal to gravity; (3) lift is equal to the centrifugal force. It is assumed that the lateral force is zero in the calculation, which is because small lateral forces have negligible effects on the entire system relative to lift and drag. So that the force equilibrium equations of the aircraft are

$$D = \frac{1}{2}\rho S V^2 C_D = mg \qquad F_c = 0 \qquad L = \frac{1}{2}\rho S V^2 C_L = m\Omega^2 R \tag{4.1}$$

The three-axis moment equations about the body axis are

$$M_i = f(I_{ij}, \omega_i, \dot{\omega}_i) \tag{4.2}$$

where $i = x, y, z$, $j = x, y, z$.
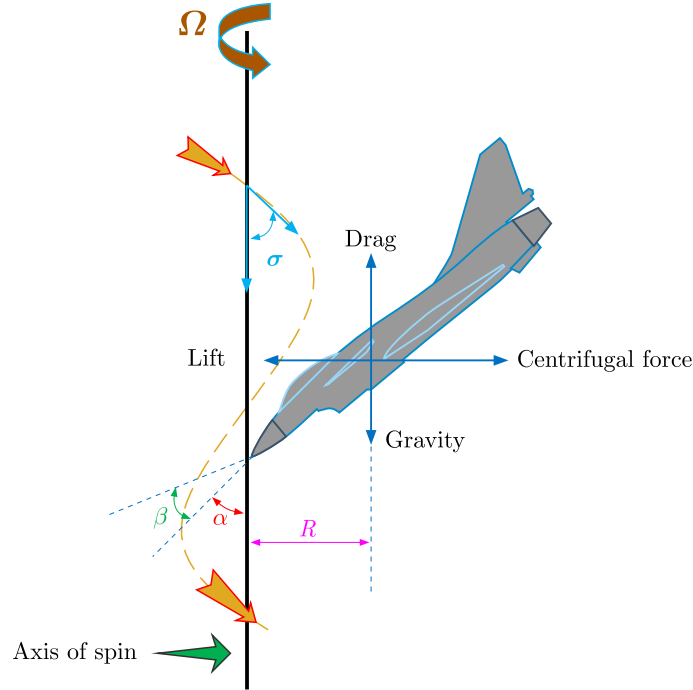
Fig. 1. Aircraft equilibrium of forces in the steady-spin

Because the longitudinal axis is the main axis of inertia in modern aircraft structures, and the cross inertial product of the symmetry plane satisfies $I_{xy} = I_{yz} = 0$, the complete body axis moment equilibrium equations can be expressed as

$$
\begin{aligned}
M_x^A &= I_{xx}\dot{\omega}_x + (I_{zz} - I_{yy})\omega_y\omega_z - I_{zx}(\omega_x\omega_y + \dot{\omega}_z) \\
M_y^A &= I_{yy}\dot{\omega}_y + (I_{xx} - I_{zz})\omega_x\omega_z + I_{zx}(\omega_x^2 - \omega_z^2) \\
M_z^A &= I_{zz}\dot{\omega}_z + (I_{yy} - I_{xx})\omega_x\omega_y + I_{zx}(\omega_y\omega_z - \dot{\omega}_x)
\end{aligned}
\tag{4.3}
$$

4.2. Motion state equations

After the aircraft enters the steady-spin, the conical rate remains constant, so

$$
\dot{\omega}_i = 0
\tag{4.4}
$$

more

$$
\omega_x = \Omega\cos\psi\cos\alpha \qquad \omega_y = \Omega\sin\psi \qquad \omega_z = \Omega\cos\psi\sin\alpha
\tag{4.5}
$$

where $\psi = -(\beta + \sigma)$, σ is the angle between the flight path and the vertical axis, and $\sigma = \arctan(R\Omega/V)$. The spin radius is generally very small when the aircraft is in the steady--spin, which makes $R \approx 0$, then $\psi \approx \beta$.

Although for the convenience of calculation, we assumed the aircraft with zero lateral force in the steady-spin, but the nose of the aircraft does not actually face the spin axis in the steady--spin. In this condition, the side slip still exists and comes from two aspects: one is that the aircraft does not face the spin axis, that β is generated; and the other is that the aircraft rotates around the spin axis and the airflow deflection produces a side slip. Although the side slip occurs, it is very small relative to the AOA, and the simulation results also confirmed this.

The general form of the moment coefficient in the steady-spin is

$$
C_i = A_j F(\mathbf{q}, \mathbf{u})
\tag{4.6}
$$

where $i = l, m, n \; j = 1, 2$, then

$$A_1 = \frac{1}{\rho S b} \qquad A_2 = \frac{1}{\rho S c} \tag{4.7}$$

and

$$\mathbf{q} = \begin{bmatrix} I_{xx} & I_{yy} & I_{zz} & I_{zx} \end{bmatrix}^{\mathrm{T}} \tag{4.8}$$

The state model of the aerodynamic moment coefficient can be obtained as follows

$$\begin{bmatrix} C_l \\ C_m \\ C_n \end{bmatrix} = \begin{bmatrix} A_1 & 0 & 0 \\ 0 & A_2 & 0 \\ 0 & 0 & A_1 \end{bmatrix} \cdot (\mathbf{u} \cdot \mathbf{q}) \tag{4.9}$$

where

$$\mathbf{u} = \begin{bmatrix} 0 & \sin(2\alpha)\cos^2\left(\beta\dfrac{\Omega^2}{V^2}\right) & -\cos\alpha\sin\left(2\beta\dfrac{\Omega^2}{V^2}\right) \\ -\sin\alpha\sin\left(2\beta\dfrac{\Omega^2}{V^2}\right) & 0 & \cos\alpha\sin\left(2\beta\dfrac{\Omega^2}{V^2}\right) \\ \sin\alpha\sin\left(2\beta\dfrac{\Omega^2}{V^2}\right) & -\sin(2\alpha)\cos^2\left(\beta\dfrac{\Omega^2}{V^2}\right) & 0 \\ -\cos\alpha\sin\left(2\beta\dfrac{\Omega^2}{V^2}\right) & 2(\cos^2\alpha - \sin^2\alpha)\cos^2\left(\beta\dfrac{\Omega^2}{V^2}\right) & \sin\alpha\sin\left(2\beta\dfrac{\Omega^2}{V^2}\right) \end{bmatrix}^{\mathrm{T}} \tag{4.10}$$

5. Simulation and result analysis

5.1. Calculation conditions

In this paper, a training aircraft is taken as an example to simulate the departure characteristics and steady-spin. The data satisfy: $0° \leqslant \alpha \leqslant 90°$, positive τ signifies clockwise rotation of the aircraft to the outside observers, and the center of gravity is the front. The left spin ($\tau < 0$) is calculated separately from the right spin ($\tau > 0$) and two different control conditions, neutral control and pro-spin control, are considered:

— Neutral control, that means $\delta_a = \delta_e = \delta_r = 0°$
— Pro-spin control, for the left spin, $\delta_e = -30°$, $\delta_r = +30°$, $\delta_a = -18°$ - $+12°$, and the same operations for the right spin. Positive δ_e and δ_a when the trailing-edge is down, positive δ_r when trailing-edge is left.

Also, it is calculated according to the maximum weight wt_{max} and the minimum weight wt_{min}, with the following conditions as shown in Table 1.

Table 1. Initial calculation conditions

Condition	Max-weight	Min-weight
m [kg]	3300	2800
I_{xx} [kg·m^2]	6200	3800
I_{yy} [kg·m^2]	15000	14500
I_{zz} [kg·m^2]	20000	17000

5.2. Simulation results and analysis

5.2.1. Departure characteristic

When predicting the departure characteristics, wt_{max} is calculated separately from wt_{min}, because the weight will cause a change of the moment of inertia. The curve of $C_{n\beta D}$-α is obtained, as shown in Fig. 2.

As can be seen from Fig. 2, $C_{n\beta D}$ in whole, positive AOA are in a steady region, whether in wt_{max} or wt_{min}, indicating that directional stability is present, and with increasing AOA, the value of $C_{n\beta D}$ increases and the directional stability is enhanced. In addition, it can also be seen that the rise of the wt_{min} curve is greater than that of wt_{max}, indicating that the directional stability under wt_{min} is better than that under wt_{max}. Therefore, it can be determined that the aircraft will not deviate from its course sharply after stalling.
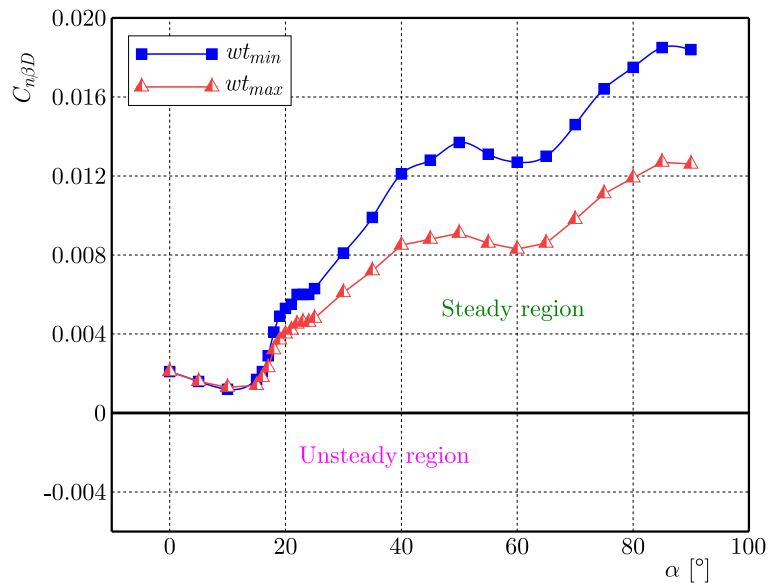
Fig. 2. $C_{n\beta D}$-α curves

5.2.2. Simulation of steady-spin characteristics

(A) Characteristics of steady-spin

After simulation, the yawing moment equilibrium curves C_{na}-C_{ni} and the corresponding curves of τ under several conditions in Section 5.1 are obtained, as shown in Fig. 3 and Fig. 4.

Figure 3 shows the yawing moment coefficient equilibrium curves and the corresponding τ for the four cases in the left spin $\tau < 0$, but not all of the curves have intersections. In Fig. 3a, the curves of the aerodynamic yawing moment and the inertial yawing moment have no intersection, but they are very close between AOA 45° and 55°, which proves that the aircraft is in a near-equilibrium state in this region. Except for this case, the curves in the other three states have intersections, especially in Fig. 3b, which has two intersections. But these two intersections may not be all that we need. The judgment of the equilibrium point will appear in the following (B).

By comparing Figs. 3a and 3b, we found that under neutral control, the curves of wt_{min} and wt_{max} are highly consistent, and the same conclusion can be drawn by comparing Figs. 3c and 3d. However, comparing Fig. 3a with Fig. 3c, the curves have changed significantly, as have Fig. 3b and 3d. In addition, the number of intersections at the curves is also changing in various ways. This is because the deflection has a great influence on the moment coefficient of the three axes, while the weight change has little effect in a small range. However, both of them will have an effect on the steady-spin characteristics.
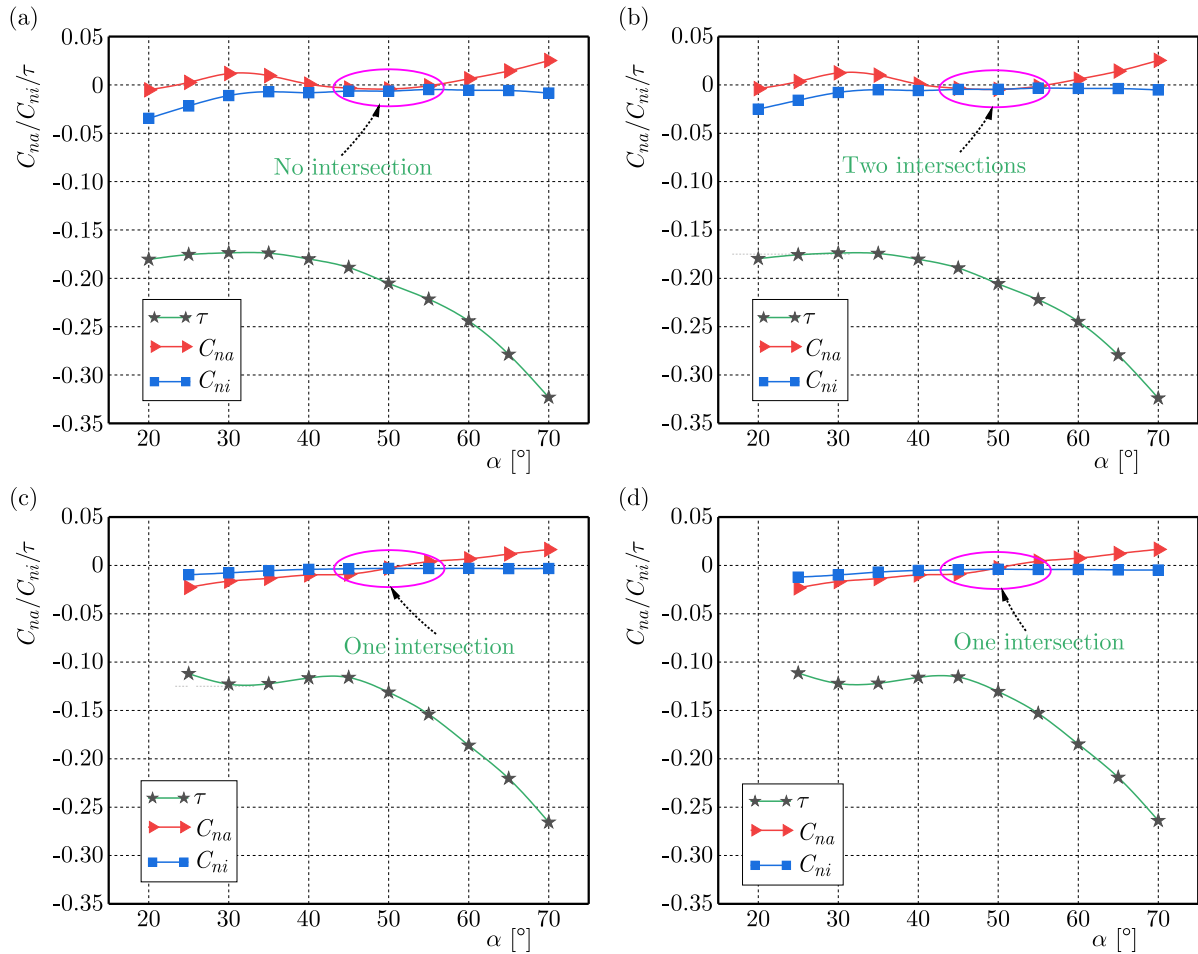
Fig. 3. The yawing moment equilibrium and τ vs α in the left spin: (a) wt_{min} and neutral control, (b) wt_{max} and neutral control, (c) wt_{min} and pro-spin control, (d) wt_{max} and pro-spin control

Similarly, as shown in Fig. 4, we obtained curves under the right spin ($\tau > 0$), with the same deflection control as the left spin. Like the left spin, the right spin also shows that the deflection has a greater influence on the moment coefficient than the weight. However, in the right spin, the curves only have two intersections (see Fig. 4c), and the curves are close to the equilibrium in other configurations between AOA 45° and 55°. Comparing Fig. 3 with Fig. 4, we can see that it is hard for the aircraft to enter the steady-spin in the right spin but easy in the left spin.

(B) Equilibrium criterion

The moment equilibrium and τ curves of the aircraft in the left and right spin were obtained in (A), and four cases of the configuration with intersections are shown in Fig. 5. Among the two intersections, there must be one intersection that we do not need, but even if there is a single intersection, it is not necessarily a solution, and the equilibrium criterion needs to be used for screening.

The criterion of steady-spin equilibrium requires that the slope of the aerodynamic moment coefficient curve at the intersection be different from the corresponding curve of τ. This occurs because the aircraft with longitudinal stability must obtain increased or decreased $|\tau|$ at a larger or smaller AOA than predicted, otherwise it will not be able to maintain pitching stability. The aerodynamic yawing moment coefficient, as a damping moment, should correspond to τ, which means that the slope of the aerodynamic yawing moment coefficient curve must be opposite to the τ curve in order to maintain stability. In the right spin, the slopes of the curves of τ at the
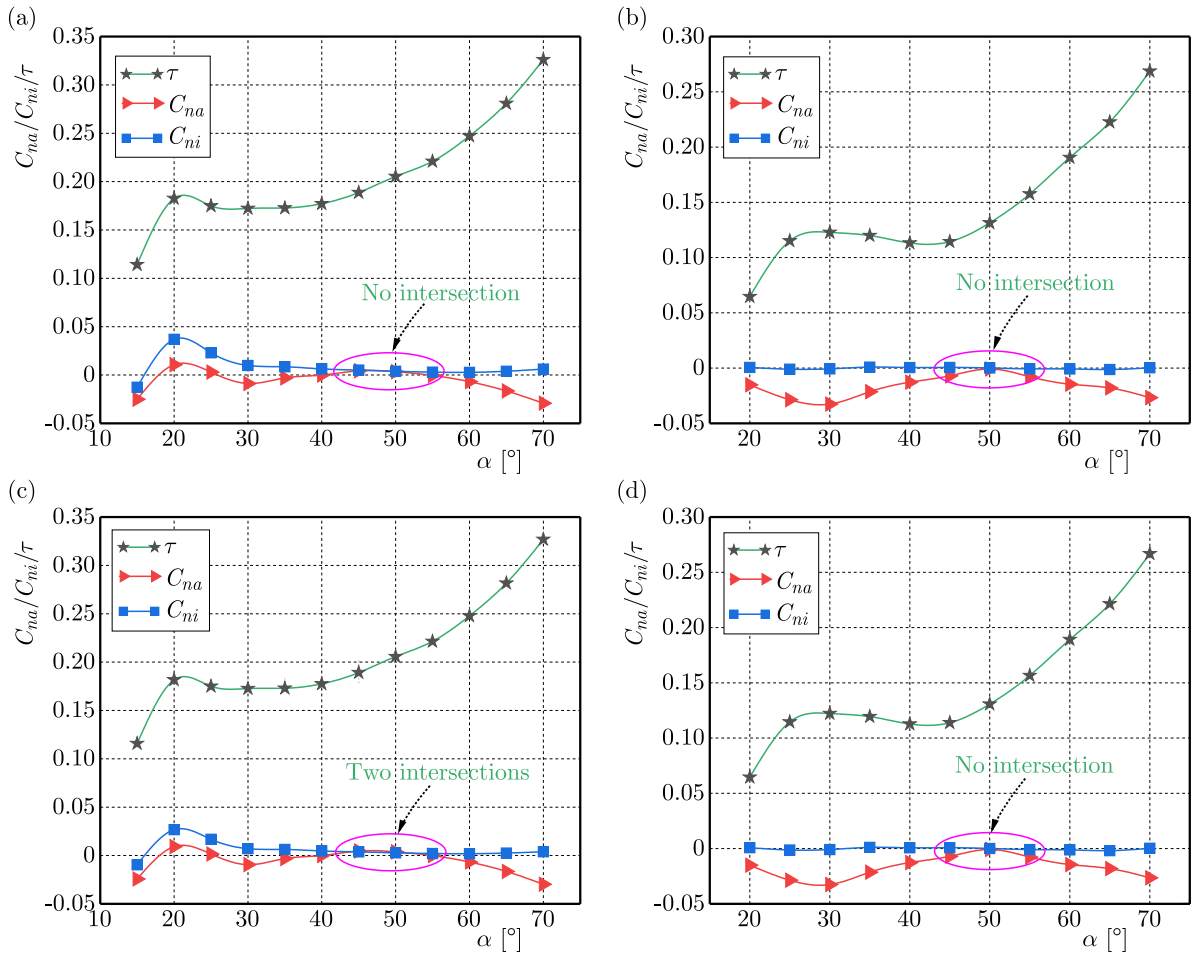
Fig. 4. The yawing moment equilibrium and τ vs α in the right spin: (a) wt_{min} and neutral control, (b) wt_{max} and pro-spin control (for the left spin), (c) wt_{max} and neutral control, (d) wt_{min} and pro-spin control (for the left spin)

intersection are all positive, so the slopes of the aerodynamic moment coefficient curves should be negative. The equilibrium point to be found in Fig. 5a is intersection II. Unlike the right spin, the slopes of the τ curves at the intersections in the left spin are negative, so the slopes of the aerodynamic moment coefficient curves should be positive. Therefore, in Fig. 5b, intersection IV meets the requirements, while the intersections in Fig. 5c and 5d both meet the criteria.

(C) Calculation of spin parameters

According to the equilibrium AOA, β and τ of steady-spin can be found out from the curves of moment equilibrium, as shown in Fig. 6. After α, β and τ are obtained, C_L and C_D in this state can be found from the test data of the rotary balance, and then V and R can be determined according to equation (4.1).

In the steady-spin, ΔH and Δt can be expressed as

$$\Delta H = \frac{\pi b}{\tau} \qquad \Delta t = \frac{\Delta H}{V} \tag{5.1}$$

Finally, all steady-spin equilibrium solutions can be obtained, which are shown in Table 2.

Although the aircraft is symmetrical, the characteristics of the left and right spin will be different. In this paper, this situation is mainly related to aerodynamic characteristics. When predicting the left and right spin of an aircraft in the steady-spin, the aerodynamic moment
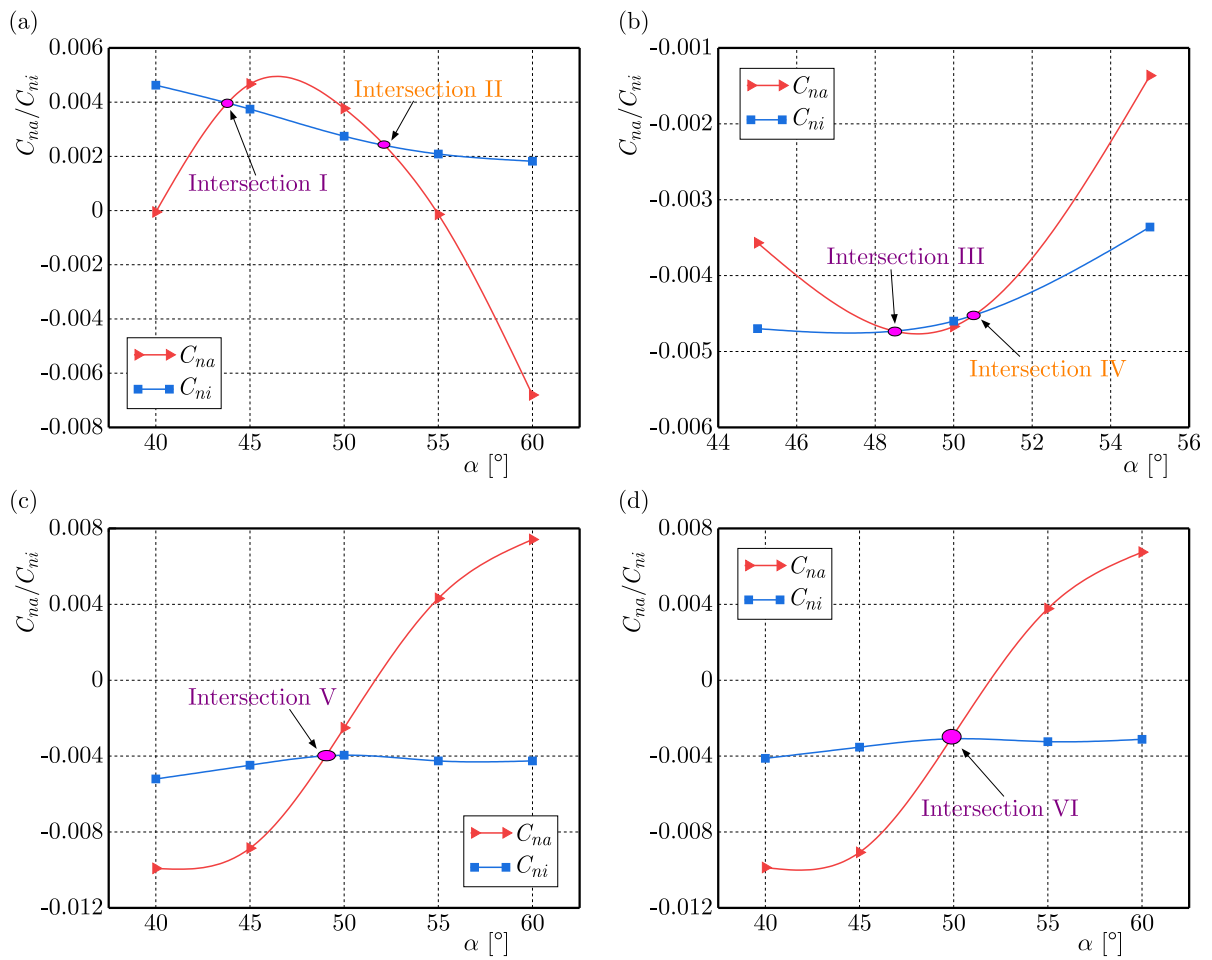
Fig. 5. Curves at the intersections: (a) wt_{max} and neutral control, in the right spin, (b) wt_{max} and neutral control, in the left spin, (c) wt_{min} and pro-spin control, in the left spin, (d) wt_{max} and pro-spin control, in the left spin
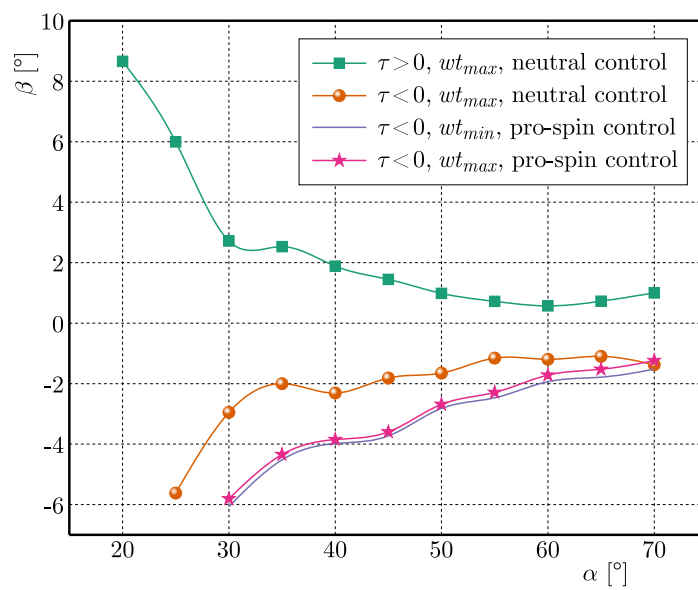
Fig. 6. β corresponding to the equilibrium points

Table 2. Complete steady-spin equilibrium solutions

	Intersection II	Intersection IV	Intersection V	Intersection VI
α [deg]	51.6	50.2	48.8	49.8
τ [−]	0.21	−0.21	−0.13	−0.13
β [deg]	0.9	−1.6	−3.0	−2.7
V [m/s]	68.5	69.8	64.7	70.2
R [m]	1.87	1.89	6.04	4.94
ΔH [m]	149	149	241	241
Δt [s]	2.2	2.1	3.7	3.4

coefficients needed are obtained from the wind tunnel test data of the rotary balance with positive and negative τ. However, under the same α, the aerodynamic moment coefficients corresponding to positive and negative τ are not necessarily symmetrical, especially at high α, which may be caused by the small asymmetry of the aircraft model, asymmetric vortex at high α, wind tunnel test equipment, and other factors.

6. Conclusion

In this paper, we can draw some conclusions:

- The departure characteristics and spin characteristics of the aircraft can be well analyzed using the wind tunnel test data; however, due to limitations of the analysis method, the simulation results will have large errors. There are many assumptions and preconditions, which will cause many subtle influencing factors to be ignored, so that the simulation results have large errors, which can only meet the initial stage of aircraft design and analysis.
- Through the static force test data at high AOA, the sideslip characteristics of the aircraft can be simulated. The obtained results show that the aircraft has good directional stability in the entire positive AOA range, and that it will improve as the AOA increases. At the same time, the directional stability of the aircraft under wt_{max} is weaker than wt_{min}.
- The influence of deflection on the steady-spin characteristics is greater than the moment of inertia, but in several different situations, the aircraft is in an equilibrium state or close to the equilibrium when AOA is about 50°.
- Among four equilibrium solutions, three appear in the left spin and only one appears in the right spin, which means that the probability of the aircraft having a steady spin in the left spin is greater than that in the right spin.
- The criterion of the steady-spin equilibrium point should be discussed according to whether the aircraft is in the left spin or the right spin. Some references have expressed that the criterion for the equilibrium point is that the slope of the aerodynamic moment curve is negative. But this situation is only for the right spin, since the slope of the τ curve for the right spin is positive, while the situation for the left spin is just opposite. It requires that the slope of the aerodynamic moment curve where the equilibrium point is located be positive in the left spin.
- The spin trajectories in different states are quite different. In intersections II and IV, $R \approx 1.8$ m, while it is 6 m in intersection V, and $\Delta H = 241$ m.

References

1. ABRAMOV N., GOMAN M., KHRABROV A., 2004, Aircraft dynamics at high incidence flight with account of unsteady aerodynamic effects, *AIAA Atmospheric Flight Mechanics Conference and Exhibit*, **5274**

2. BENNETT C.J., LAWSON N.J., 2018, On the development of flight-test equipment in relation to the aircraft spin, *Progress in Aerospace Sciences*, **102**, 47-59

3. BIHRLE JR W., BARNHART B., 1983, Spin prediction techniques, *Journal of Aircraft*, **20**, 2, 97-101

4. CHAMBERS J.R., 1969, Analysis of lateral-directional stability characteristics of a twin-jet fighter airplane at high angles of attack, *NASA TN D-5361*

5. CHURKIN A., BIALEK J., POZO D., SAUMA E., KORGIN N., 2021, Review of cooperative game theory applications in power system expansion planning, *Renewable and Sustainable Energy Reviews*, **145**, 111056

6. COLLINS J., SABLE A., 2015, *Stall and Spin Accidents: Keep the Wings Flying*, AOPA Air Safety Institute

7. CUMMINGS R.M., LIERSCH C., SCHUETTE A., 2018, Multi-disciplinary design and performance assessment of effective, agile NATO air vehicles, *2018 Applied Aerodynamics Conference*, 2838

8. FARCY D., KHRABROV A.N., SIDORYUK M.E., 2020, Sensitivity of spin parameters to uncertainties of the aircraft aerodynamic model, *Journal of Aircraft*, **57**, 922-937

9. FIGAT M., GORAJ Z., 2016, Analysis of stability derivatives important to recovery from spin, *Aviation*, **20**, 2, 48-52

10. IGNATYEV D.I., KHRABROV A.N., 2015, Neural network modeling of unsteady aerodynamic characteristics at high angles of attack, *Aerospace Science and Technology*, **41**, 106-115

11. KAPUSCINSKI T., SZCZERBA P., ROGALSKI T., RZUCIDLO P., SZCZERBA Z., 2020, A vision-based method for determining aircraft state during spin recovery, *Sensors (Basel)*, **20**, 8, 2401

12. KOU J., ZHANG W., 2021, Data-driven modeling for unsteady aerodynamics and aeroelasticity, *Progress in Aerospace Sciences*, **125**, 100725

13. LEE S., CHOI Y., CHUNG H.S., 2019, Forced oscillation wind tunnel tests for dynamic characteristic of aircraft, *AIAA Aviation 2019 Forum*

14. MALIK B., AKHTAR S., MASOOD J., 2017, Influence of flight control law on spin dynamics of aerodynamically asymmetric aircraft, *Journal of Theoretical and Applied Mechanics*, **55**, 963-975

15. MOKHTARI M.A., SABZEHPARVAR M., 2018, Identification of spin maneuver aerodynamic nonlinear model by applying ensemble empirical mode decomposition and extended multipoint modeling, *Proceedings of the Institution of Mechanical Engineers, Part G: Journal of Aerospace Engineering*, **233**, 1865-1878

16. ROGALSKI T., RZUCIDŁO P., PRUSIK J., 2020, Unmanned aircraft automatic flight control algorithm in a spin maneuver, *Aircraft Engineering and Aerospace Technology*, **92**, 8, 1215-1224

17. SIBILSKI K., WRÓBLEWSKI W., 2012, Prediction of aircraft spin characteristics by continuation and bifurcation methods, *AIAA Atmospheric Flight Mechanics Conference*, **4799**

18. STENFELT G., RINGERTZ U., 2013, Yaw departure and recovery of a tailless aircraft configuration, *Journal of Aircraft*, **50**, 311-315